URN (Paper): urn:nbn:de:gbv:ilm1-2014iwk-114:4

INSERT WITH A MULTIPLE FIXED-POINT CELL FOR A DRY BLOCK CALIBRATOR

S. Marin, M. Hohmann, M. Schalles, G. Krapf, T. Fröhlich

Technische Universität Ilmenau, Institute for Process Measurement and Sensor Technology,
POB 100565, 98684 Ilmenau

ABSTRACT

The thermal design of a multiple fixed-point cell for use in a dry block calibrator was developed at the Technische Universität Ilmenau. The design was made using thermal Finite Element simulations with ANSYS Workbench and parametrical studies with optiSLang. The multiple fixed-point cell contains three pure materials, with melting and freezing temperatures within the block calibrator`s working range from room temperature to 600 °C. They enable an in-situ calibration of the block reference temperature sensor at the phase transition temperatures of the materials. This paper shows different geometries of the fixed-point cell, their optimization, melting curves and temperature field calculations for the estimation of the best design.

Index Terms **–** dry block calibrator, in-situ calibration, multiple fixed-point cell, thermal finite element simulation, parametrical study

1. INTRODUCTION

The calibration of temperature sensors in industry is mainly carried out by comparison calibrations, where the reference sensor and the sensor under test are brought to the same temperature in a calibration bath or in dry block calibrator. The first type of devices allows a calibration with a low uncertainty in a limited temperature range because of the working fluid. Calibrations with the second type of devices have a higher uncertainty due to the stem error and the thermal coupling between the insert and the sensor under test but allow higher working temperatures [1]. Both devices have an internal reference sensor, which has to be removed for calibration. Instead of the internal sensor, a calibrated external sensor can be used to achieve a lower calibration uncertainty.

A new dry block calibrator was built at the Institute for Process Measurement and Sensor Technology of Technische Universität Ilmenau which is equipped with a multiple fixed-point cell with three fixed-point materials according to the International Temperature Scale (ITS-90). Their freezing temperatures, called fixed-points temperatures, are used for traceable in-situ calibrations according to the ITS-90 for the reference sensor well as for the sensor under test. The fixed-point temperatures are within the working range of the dry block calibrator from room temperature up to 600 °C. By performing that in-situ calibration, the removal of the reference sensor and the use of an external sensor for calibration are avoided.

The new dry block calibrator´s operating principle is based upon Fourier´s law of heat conduction [2]. It says that a heat flux inside a body is driven by a thermal gradient. This relations means that there are no thermal gradients inside the body if there is no heat flux. The block calibrator includes a nickel coated copper block split into three parts (1, **Figure 1**),

called insert, three self-designed heat flux sensors (2), two between the insert parts and one additionally below them. Electrical heaters (3) are distributed around the insert. They are used to adjust the temperature of the insert parts. For that, the heaters are controlled in a manner that the heat flux through the heat flux sensors is zero, thus there are no thermal gradients in axial direction. The block calibrator moreover contains three external heaters (4) providing an adiabatic shield between the insert and the ambiance to reduce the temperature gradients in radial direction. The entire block is furthermore isolated from the ambiance with an insulation material (5). Between the external and internal heaters is a gap which can be purged with air to cool down the calibrator (6).

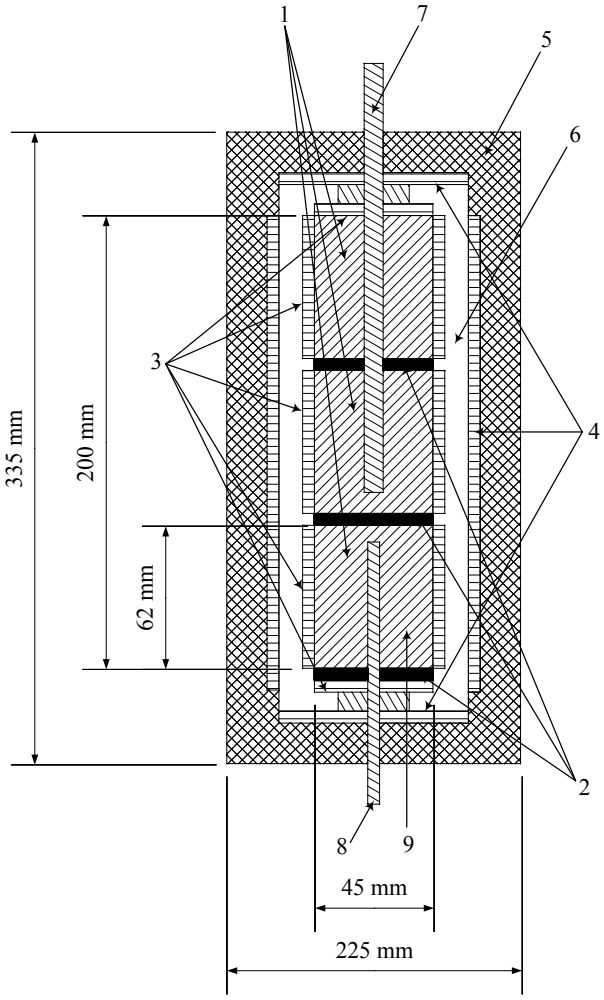

***Figure 1**- New block calibrator with heat flux sensors and an adiabatic shield.*

The sensor under test (7) and the reference sensor (8) are coaxial aligned to be homogeneously tempered in radial direction. The insert part at the bottom (9), wherein the reference sensor is inserted, can be replaced with a multiple fixed-point cell. To assure a traceable calibration of the reference sensor at the cell's fixed-points temperatures the design of the cell needs to be optimized. Here, possible geometrical shapes of the cell and different arrangements of the fixed-point materials in the cell were investigated to find its best temperature field.

2. MULTIPLE FIXED-POINT CELL

For an in-situ and traceable calibration a multiple fixed-point cell was included in the insert of the dry block calibrator. The reference sensor is calibrated by the three fixed-points temperatures and the sensor under test is calibrated by comparison with the reference sensor. The fixed-points are equilibrium states between the pure materials liquid and solid phases (melting and freezing points). The temperature of these points is constant and reproducible with a low uncertainty. The materials and their fixed-point temperatures are defined in the ITS-90 [3]. The three materials indium, tin and zinc were selected for the cell. These materials have their fixed-point temperature in the working range of the dry block calibrator (**Table 1**).

When the dry block calibrator is heated up and cooled down afterwards using a well defined heating procedure, one can induce three consecutive melting (m) and freezing (f) processes. During these processes, the temperature in the multiple fixed-point cell develops as it is shown schematically in **Figure 2**. The length of the temperature plateaus depends on the heating or cooling regime and on the material's latent heat (energy released or absorbed by a body during a constant-temperature process).

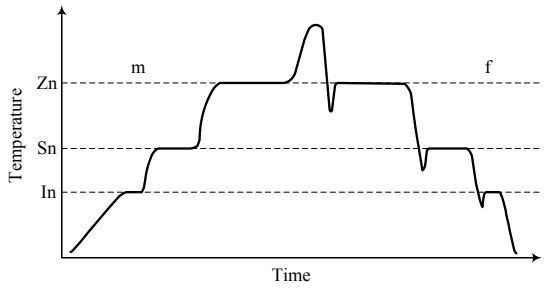

***Figure 2** - Schematic diagram of a temperature measurement three fixed-points.*

***Table 1** - Selected fixed-point materials for the cell.*

material	fixed-point temperature at atmospheric pressure (°C)
indium, In	156.5985
tin, Sn	231.928
zinc, Zn	419.527

Another material of the ITS-90 which possibly could be used in the range is Gallium. It was not taken into account because its fixed-point temperature (29.7646 °C) is close to the room temperature and liquid Gallium needs a supercooling of several Kelvin under its fixed-point temperature to freeze. Since the dry block calibrator can only be cooled to room temperature, reaching the freezing point of Gallium would be difficult.

2.1 Geometrical design

For the cell design three different geometries with fixed-point materials in coaxial arrangement were selected. They are called models (**Figure 3**). From former research it is known, that these arrangements achieve a good starting point to optimize due to their temperature field [4]. The best model was estimated by means of parametrical studies. For this, geometrical parameters were defined (a to h, **Figure 3**), and were varied regarding the dimensions of the insert part (9, **Figure 1**) by means of Finite Element Simulations (FEM). The positions of the fixed-point materials in the cell (in, ctr, out, **Figure 3**) were varied as well. Graphite was selected as material for the crucible of the fixed-point cell, because of its high thermal conductivity, the chemical compatibility with the fixed-point materials and its good processability compared with ceramic materials.

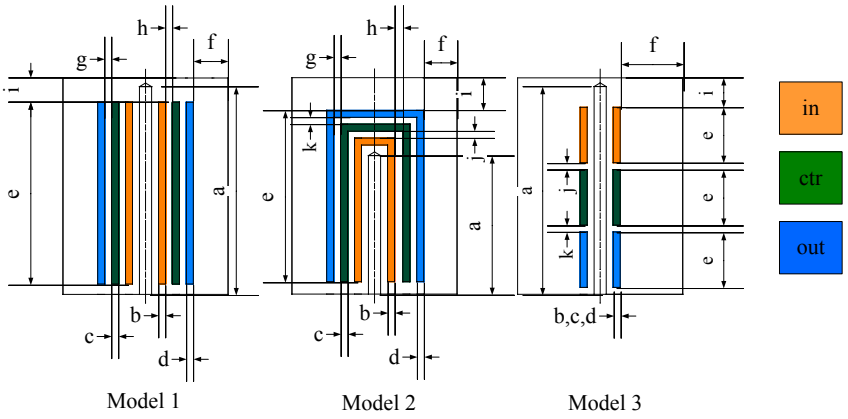

Figure 3 *- Fixed-point cell arrangements and the parameters for the parametrical study.*

2.2 Numerical model

The block calibrator was modeled for the simulation as an axially symmetrical model (**Figure 4**) in ANSYS Workbench. The mesh was refined until it had no influence on the temperature results of a simulation, thus the results are mesh independent.

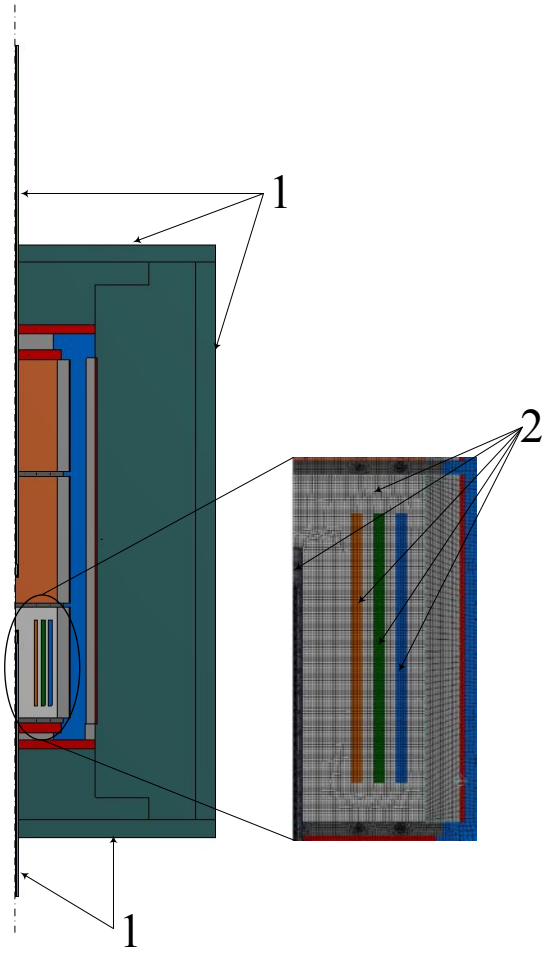

Figure 4 *- Block calibrator´s axially symmetrical model with energy outputs (1) and mesh*

2.2.1 Boundary conditions

The energy input by the heaters (3, 4, **Figure 1**) and the heat loss to ambiance due to convection (1, **Figure 4**) were estimated theoretically [2]. During a calibration the cooling by air is not activated. That's because the air was assumed to be mainly thermally conducting. Here, an equivalent thermal conductivity of the air was calculated according to **Equation 1** which additionally takes into consideration the radiation heat exchange in the air gap. This helps to reduce the computation time, compared to a simulation with a separate definition of the radiation heat exchange.

Equation 1

$$\lambda_{equ} = \lambda + \left[4 \cdot \sigma \cdot r_1 \cdot r_2 \cdot \ln\left(\frac{r_2}{r_1}\right) \cdot T_m^{\,3} \right]$$

λ_{equ} = Equivalent thermal conductivity of air including radiation / $W \cdot m^{-1} \cdot K^{-1}$
λ = Thermal conductivity of air / $W \cdot m^{-1} \cdot K^{-1}$
σ = Stefan - Boltzmann constant / 5.67 x 10^{-8} $W \cdot m^{-2} \cdot K^{-4}$
r_1 = Radius of the internal conduct / m
r_2 = Radius of the external conduct / m
T_m = Mean temperature between both conducts / K

2.2.2 Material properties

The thermal properties of the materials were defined, if possible, as temperature dependent. **Table 2** shows the used materials with their thermal properties at a temperature of 25 °C.

***Table 2** - Thermal material properties at 25 °C used in the simulations [5–8].*

material	density ρ ($kg \cdot m^{-3}$)	thermal conductivity λ ($W \cdot m^{-1} \cdot K^{-1}$)	specific heat capacity c ($J \cdot kg^{-1} \cdot K^{-1}$)	fixed-point temperature (°C)	latent heat L ($J \cdot g^{-1}$)	thermal diffusivity α ($m^2 \cdot s$)
air	1.168	$25.73 \cdot 10^{-3}$[a]	1007	-	-	
alumina	3800	35	900	-	-	
copper	8910	310	370	-	-	
glass ceramic	2660	1.72	789	-	-	
graphite	1840	90	708	-	-	
heater wire	7100	11	460	-	-	
insulation	300	0.09[b]	1050	-	-	
magnesia	3400	7	850	-	-	
stainless steel	7900	15	500	-	-	
platinum	21450	72	134	-	-	
indium	7283	82	233	156.5985	28	$4.8 \cdot 10^{-5}$
tin	7290	67	227	231.928	59	$4.0 \cdot 10^{-5}$
zinc	7133	116	388	419.527	112	$4.2 \cdot 10^{-5}$

[a]Equivalent thermal conductivity of air (**Equation 1**). [b]Thermal conductivity value at 400 °C.

2.3 Thermal design

The aim of the design optimization is to find a cell geometry and an arrangement of the fixed-point materials which has the lowest thermal gradients between the cell and the reference sensor during a phase transition. Ideally, the phase transition temperature at each fixed-point and the reference sensor temperature should be equal and constant in time. Furthermore the temperature plateau during the phase change should be flat and the sensor response time should be small.

Three models for the in-situ calibration were compared. For this purpose, at first steady state simulations in a parametrical study were made to find the best model, geometry and fixed-point materials position. After that, transient simulations of the best model were made to check the flatness of the plateaus and the response time of the sensor.

3. THERMAL SIMULATIONS

3.1 Steady state simulation

The steady state simulation was made in three steps. It was supposed at each step, that one entire fixed-point material (In, Sn, Zn) is at the fixed-point temperature (**Table 1**) and the heaters (3, 4, **Figure 1**) are at a temperature 2K higher than the respective fixed-point temperature. To compare the results, the sum of the maximum temperature difference in the cell and in the reference sensor was estimated for each step (2, **Figure 4**), (**Equation 2**).

Equation 2
$$\Delta\vartheta_T = (\vartheta_{max} - \vartheta_{min})_T = (\vartheta_{max} - \vartheta_{min})_{In} + (\vartheta_{max} - \vartheta_{min})_{Sn} + (\vartheta_{max} - \vartheta_{min})_{Zn}$$

$\Delta\vartheta_T$ = Sum of the maximal temperature difference on the block and on the temperature sensor for each fixed-point / °C
ϑ_{max} = Maximum temperature of the cell and of the temperature sensor / °C
ϑ_{min} = Minimum temperature of the cell and of the temperature sensor / °C

For sensitivity analysis and optimization the software optiSLang was used. This tool calculates response surfaces by means of polynomial regression with the simulations results and measures its quality for the full model and the importance of each input parameter on the outputs parameters with the Coefficient of Prognosis CoP [9]. When the CoP is greater than 70%, the model is described well enough. To obtain these response surfaces, the geometrical parameters and the position of the fixed-point materials in the cell for each model were varied (**Figure 3**). In this analysis, the parameters with the greatest influence on the output variable, in this case $\Delta\vartheta_T$ (**Equation 2**), were estimated. After this, the best geometrical dimensions and the best arrangement of the fixed-point materials for a minimum of $\Delta\vartheta_T$ were searched in the calculated response surfaces. Since the optimization was performed by optiSLang, the calculated results will not be equal to the ANSYS calculated results. This would require a CoP of 100% (**Table 4**).

3.1.1 Results

Table 3 shows the selected parameters by optiSLang, the CoPs for the full model and for each input parameter, the initial values and the optimal parameter values for each model. The CoP percent value shows the input parameters influence on the output parameter. The greater the value the higher is the influence.

The models 1 and 2 are mostly influenced by the fixed-point length (parameter e). The model 3 is mainly influenced by the horizontal distance from the external fixed-point material to the crucible outer face (parameter f). **Figure 6** shows the response surface for the two most relevant input parameters on $\Delta\vartheta_T$.

Table 3 *- Selected geometrical and thermal parameters of each model after the sensitivity analysis with $\Delta\vartheta_T$ as output parameter*

ref	parameter	modell 1 CoP (%)	modell 1 initial value	modell 1 optimized value	modell 2 CoP (%)	modell 2 initial value	modell 2 optimized value	modell 3 CoP (%)	modell 3 initial value	modell 3 optimized value
a	imm_depth	28	23 mm	13 mm	6	23 mm	20 mm	14	13 mm	25.3 mm
e	length	68	40 mm	48.5 mm	51	40 mm	40 mm	4	11 mm	5 mm
f	h_out_out	5	5 mm	3.25 mm	9	5 mm	3.25 mm	47	15 mm	4.9 mm
i	v_out_out	33	10 mm	7 mm	-	-	-	5	10 mm	26.6 mm
j	v_out_ctr	-	-	-	-	-	-	5	3 mm	1 mm
	in	-	-	-	-	-	-	10	157 °C	232 °C
	ctr	5	232 °C	232 °C	2	-	-	10	232 °C	157 °C
	out	3	420 °C	420 °C	3	420 °C	420 °C	-	-	-
CoP full model (%)			90			70			83	

The results from the response surfaces were again simulated in ANSYS and compared in **Table 4**. optiSLang describes the ANSYS models very well, hence the relative difference is very small. For example, for the model with the poorest description, model 2, the difference is 6%, although CoP is only 70%. The model with the best output parameter $\Delta\vartheta_T$ after the optimization is model 1. Its temperature field is very homogeneous during the phase transitions. **Figure 5** shows the simulated temperature field of the three optimized models at the indium fixed-point. The position of In is in the inner cavity (in, **Figure 3**) at model 1 and model 2 and in the middle cavity at model 3 (ctr, **Figure 3**).

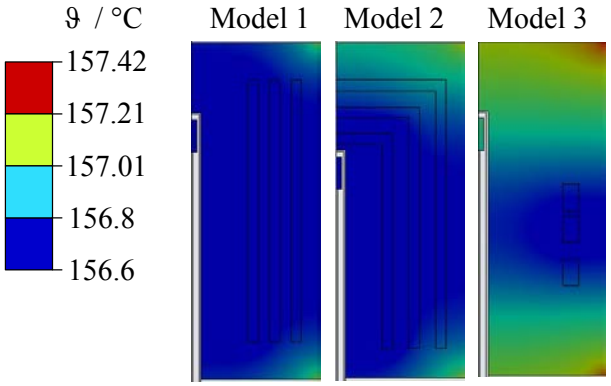

Figure 5 *- Temperature field for the optimized models during indium´s phase change.*

3.1.2 Position of the fixed-point materials in the cell for the Model 1

For the steady state optimization, the thermal conductivity and the volume of each fixed-point material was taken into account. Here, the best results were found for the material arrangement indium - tin - zinc (from inner to outer position inside the cell). An optimization for the transient case must also include the thermal diffusivity and the latent heat of the material. The zinc is filled in the exterior cavity with the greatest volume. Its latent heat is greater and its thermal diffusivity is lower compare to indium. Thus, fast temperature variations on the heaters should not affect the phase transition very strong. The indium cavity is protected against temperature variations of the ambiance during its phase transition by the other fixed-point materials. These considerations lead to the conclusion, that that the optimal cell arrangement of the steady state is the best for the dynamic case as well.

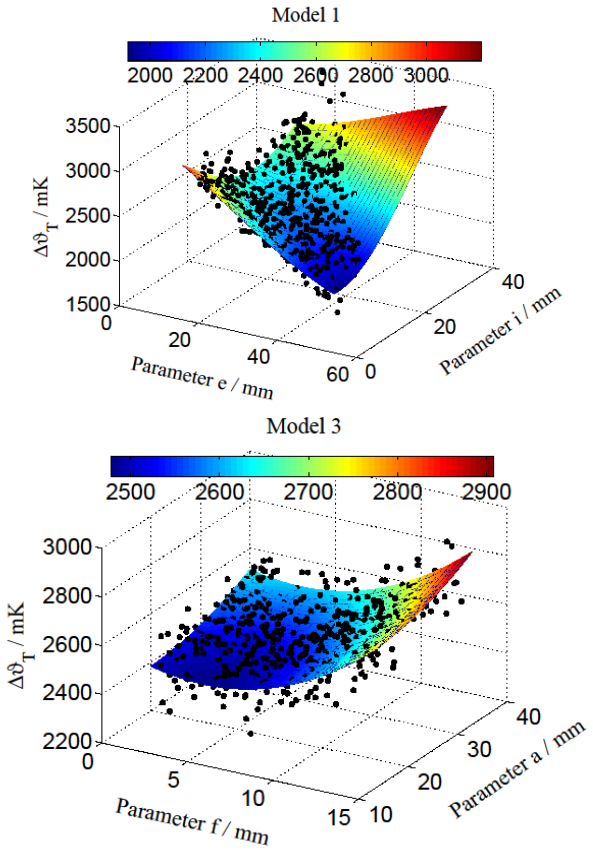

***Figure 6** - Polynomial regression response surface for the most influencing input parameters. The black points show the simulated values.*

	$\Delta\vartheta_T$ (mK)		
	Modell 1	**Modell 2**	**Modell 3**
ANSYS	1620	1695	2562
optiSLang	1605	1803	2501
relative difference (%)	1	6	2

***Table 4** - $\Delta\vartheta_T$ for each optimized model simulated and from the optiSLang´s response surfaces.*

3.2 Transient Simulation

After the cell optimization, transient simulations were carried out in ANSYS. They are used to investigate the real behavior of the cell during the phase transition. In the steady state simulations was assumed, that the entire fixed-point material is at fixed-point temperature, which is a hypothetical case. Thus, the flatness of the plateau and the sensor response time for the selected model in transient simulations were estimated. For this, the parameters whose influence on $\Delta\vartheta_T$ in the selected model is small were varied. These parameter were filtered in the sensitivity analysis (b, c, d, g, h **Figure 3**), hence the model temperature field (**Figure 5**) should not be strong affected. An optimization for a transient case with optiSLang would take a lot of time, consequently only three variants were defined: A is the optimized model, B has wider cavities (parameters b, c, d, **Figure 3**) and C has wider cavities (parameters b, c, d, **Figure 3**) and wider separation between the cavities (parameters g, h, **Figure 3**). **Table 5** shows the values of the parameters for each variant.

***Table 5** - Optimized variants of model 1 with a change on those parameters with small influence on $\Delta\vartheta_T$*

Parameter	Variant A	Variant B	Variant C
b	2	4	3
c	2	4	3
d	2	3.5	3
g	2	2	3.5
h	2	2	3.5

The melting process of each fixed-point material was simulated separately for a heating rate of 0.1 K/min.

3.2.1 Results

Figure 7 shows the melting plateaus and **Figure 8** shows the temperature difference between the reference sensor and the maximum temperature in the fixed-point material for the fixed-point of indium, tin and zinc respectively. The flatness of the plateaus depends on the width of the cavity. The greater the volume, the longer the duration of the phase transition. The response time of the reference sensor was defined as the time span in which the minimum temperature difference between sensor and fixed-point materials during the melting phase is reached. It is similar for the three variants, but the mean temperature gradients at this time are the smallest for variant B.

Figure 9 shows the temperature field of indium in the middle of the melting plateau (1500 s, **Figure 7**) for the three variants in comparison to model 1 in steady state. Although the entire fixed-point cell does not have the same temperature at the transient case, its temperature field is very close to the steady state field. This shows, that die optimization in steady state is a good approach.

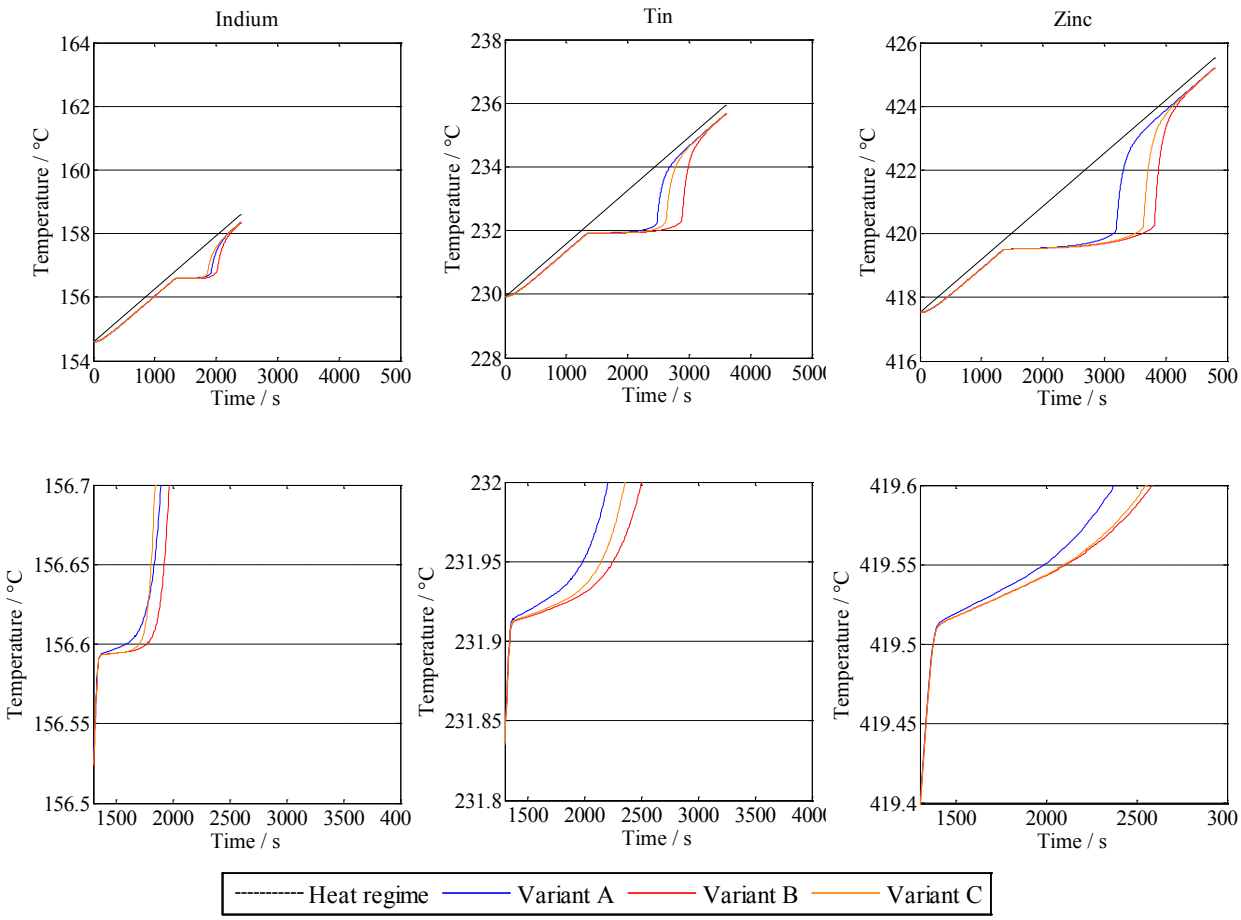

***Figure 7** – Simulated temperature at the reference sensor while melting.*

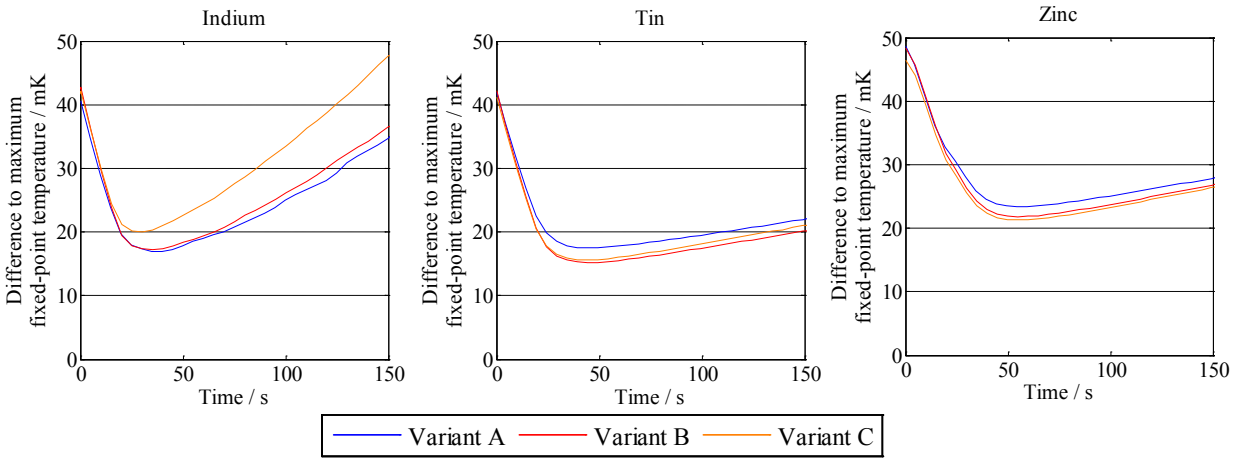

Figure 8 *- Response of the reference sensor to the melting of the fixed-point materials.*

Variant A has the best temperature distribution during the phase transition of indium, but variant B has better distributions for tin and zinc compared to variants A and C (**Figure 8**). Moreover the flattest plateaus and the quickest response time are reached with the variant B. Based on the previous reasons and on the steady state optimization, model 1 variant B is found to be the best option for the fixed-point cell.

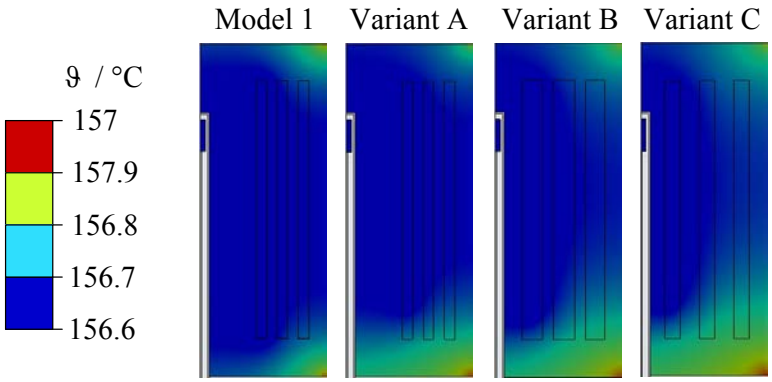

Figure 9 *- Temperature field of the optimized model 1 and its variants during indium's melting.*

4. SUMMARY

A multiple fixed-point cell for in-situ calibration in a dry block calibrator was developed and optimized by means of FEM simulations and sensitivity analyses. The cell was filled with the three fixed-points materials indium, tin and zinc, which have their melting temperature in the working range of the dry block calibrator. The cell, which enables a calibration of a thermometer traceable, was optimized by three thermal criteria: minimum temperature gradients in the cell during the phase transition of the fixed-point material, the flatness of the melting plateau and the response time of the temperature reference sensor to the phase transition of the fixed-point materials. The best arrangement of the fixed-point materials in the cell and the best cell geometry for that application were found in this work.

Acknowledgments
The authors acknowledge the financial support by the German Federal Ministry of Education and Research (BMBF) of of the VIP-Project "TempKal", in which context this work was made.

REFERENCES

[1] F. Bernhard, Technische Temperaturmessung. Springer, Berlin, 2004.
[2] M. Hohmann et al, “Metall-Blockkalibrator mit Wärmestromsensoren und adiabatischem Schild,” Sensoren und Messsysteme 2014: Beiträge der 17. GMA/ITG-Fachtagung vom 3. bis 4. Juni in Nürnberg. VDE-Verlag, Berlin, 2014.
[3] Preston-Thomas H. “The International Temperature Scale of 1990 (ITS-90),” Metrologia 27(107): 3–10, 1990
[4] M. Schalles, F. Bernhard, “Triple-Fixed-Point Blackbody for the Calibration of Radiation Thermometers,” International Journal of Thermophysics 28(6): 2049–2058, 2007.
[5] I. Barin, F. Sauert, Thermochemical data of pure substances. VCH, Weinheim, 1989.
[6] I.S. Grigoriev, E.Z Mejlichov (eds), Handbook of physical quantities. CRC Press, Boca Raton, Florida, 1997.
[7] J. Shackelford, W. Alexander (eds), CRC Materials Science and Engineering Handbook, Cambridge, 1992.
[8] S. Kabelac, VDI-Wärmeatlas. Berechnungsblätter für den Wärmeübergang, 10th edn. Springer, Berlin [u.a.], 2006.
[9] Dynardo GmbH, Methods for multi-disciplinary optimization and robustness analysis, Weimar, 2012.

CONTACTS

Ing. S. Marin sebastian.marin@tu-ilmenau.de
Prof. Dr.-Ing. habil. T. Fröhlich thomas.froehlich@tu-ilmenau.de